Key Points:

- Coherent ozone trend analysis methodology applied to multi-decade, pan-Arctic surface and ozonesonde datasets and multi-model medians
- Increasing winter Arctic tropospheric ozone overestimated by models in the free troposphere, and spring surface changes not captured
- Spring (summer) decreases (increases) in observed ozone throughout the troposphere, not always simulated by models

Correspondence to:

K. S. Law,
Kathy.Law@latmos.ipsl.fr

Author Contributions:

Conceptualization: Kathy S. Law, Jens L. Hjorth, Jakob B. Pernov, Cynthia H. Whaley, Henrik Skov, Martine Collaud Coen, Joakim Langner, Stephen R. Arnold

Arctic Tropospheric Ozone Trends

Kathy S. Law[1] , Jens L. Hjorth[2], Jakob B. Pernov[2,3] , Cynthia H. Whaley[4] , Henrik Skov[2] , Martine Collaud Coen[5], Joakim Langner[6] , Stephen R. Arnold[7] , David Tarasick[8], Jesper Christensen[2], Makoto Deushi[9] , Peter Effertz[10,11] , Greg Faluvegi[12,13] , Michael Gauss[14], Ulas Im[2], Naga Oshima[9] , Irina Petropavlovskikh[10,11] , David Plummer[4], Kostas Tsigaridis[12,13] , Svetlana Tsyro[14], Sverre Solberg[15], and Steven T. Turnock[7,16]

[1]Sorbonne Université, LATMOS-IPSL, UVSQ, CNRS, Paris, France, [2]Department of Environmental Science, Interdisciplinary Centre for Climate Change, Aarhus University, Roskilde, Denmark, [3]Extreme Environments Research Laboratory, École Polytechnique Fédérale de Lausanne, Sion, Switzerland, [4]Canadian Centre for Climate Modeling and Analysis, Environment and Climate Change Canada, Victoria, BC, Canada, [5]Federal Office of Meteorology and Climatology, MeteoSwiss, Payerne, Switzerland, [6]Swedish Meteorological and Hydrological Institute, Norrköping, Sweden, [7]School of Earth and Environment, Institute for Climate and Atmospheric Science, University of Leeds, Leeds, UK, [8]Air Quality Research Division, Environment and Climate Change Canada, Toronto, ON, Canada, [9]Meteorological Research Institute, Japan Meteorological Agency, Tsukuba, Japan, [10]Cooperative Institute for Research in Environmental Sciences (CIRES), University of Colorado, Boulder, CO, USA, [11]ESRL Global Monitoring Laboratory, National Oceanic and Atmospheric Administration (NOAA), Boulder, CO, USA, [12]NASA Goddard Institute for Space Studies, New York, NY, USA, [13]Center for Climate Systems Research, Columbia University, New York, NY, USA, [14]Norwegian Meteorological Institute, Oslo, Norway, [15]Norwegian Institute for Air Research (NILU), Kjeller, Norway, [16]Met Office Hadley Centre, Exeter, UK

Abstract Observed trends in tropospheric ozone, an important air pollutant and short-lived climate forcer (SLCF), are estimated using available surface and ozonesonde profile data for 1993–2019, using a coherent methodology, and compared to modeled trends (1995–2015) from the Arctic Monitoring Assessment Program SLCF 2021 assessment. Increases in observed surface ozone at Arctic coastal sites, notably during winter, and concurrent decreasing trends in surface carbon monoxide, are generally captured by multi-model median trends. Wintertime increases are also estimated in the free troposphere at most Arctic sites, with decreases during spring months. Winter trends tend to be overestimated by the multi-model medians. Springtime surface ozone increases in northern coastal Alaska are not simulated while negative springtime trends in northern Scandinavia are not always reproduced. Possible reasons for observed changes and model performance are discussed including decreasing precursor emissions, changing ozone dry deposition, and variability in large-scale meteorology.

Plain Language Summary The Arctic is warming much faster than the rest of the globe due to increases in carbon dioxide, and other trace constituents like ozone, also an air pollutant. However, improved understanding is needed about long-term changes or trends in Arctic tropospheric ozone. A coherent methodology is used to identify trends in surface and regular profile measurements over the last 20–30 years, and results from six chemistry-climate models. Increases in observed ozone are found at the surface and in the free troposphere during winter in the high Arctic. Paradoxically, decreases in nitrogen oxide emissions at mid-latitudes appear to be leading to increases in ozone during winter, but associated increases in Arctic tropospheric ozone tend to be overestimated in the models. Increases are also found at the surface in northern Alaska during spring but not reproduced by the models. The causes are unknown but could be related to changes in local sources or sinks of Arctic ozone or in large-scale weather patterns. Declining mid-latitude emissions, or increased dry deposition to northern forests, may explain negative surface ozone trends over northern Scandinavia in spring that are not always captured by the models. Further work is needed to understand changes in Arctic tropospheric ozone.

1. Introduction

Tropospheric ozone (O_3) is a short-lived climate forcer (SLCF) contributing to global and Arctic warming (AMAP, 2015; Sand et al., 2016; von Salzen et al., 2022), and a critical secondary air pollutant, detrimental to human health (Anenberg et al., 2010) and ecosystems (Arnold et al., 2018). The Arctic tropospheric O_3 budget is complex, as recently discussed in a companion paper, Whaley et al. (2023). It originates from photochemical

Data curation: Jens L. Hjorth, Jakob B. Pernov, Cynthia H. Whaley, Henrik Skov, Martine Collaud Coen, David Tarasick, Jesper Christensen, Makoto Deushi, Peter Effertz, Greg Faluvegi, Michael Gauss, Ulas Im, Naga Oshima, Irina Petropavlovskikh, David Plummer, Kostas Tsigaridis, Svetlana Tsyro, Sverre Solberg, Steven T. Turnock
Formal analysis: Jens L. Hjorth, Jakob B. Pernov, Cynthia H. Whaley, Henrik Skov, Martine Collaud Coen, David Tarasick, Peter Effertz, Irina Petropavlovskikh, Sverre Solberg
Investigation: Kathy S. Law, Jens L. Hjorth, Jakob B. Pernov, Cynthia H. Whaley, Henrik Skov, Martine Collaud Coen, Joakim Langner, Stephen R. Arnold
Software: Jens L. Hjorth, Jakob B. Pernov, Martine Collaud Coen
Visualization: Jens L. Hjorth, Jakob B. Pernov, Cynthia H. Whaley, Henrik Skov, Martine Collaud Coen, David Tarasick
Writing – original draft: Kathy S. Law, Jens L. Hjorth, Jakob B. Pernov, Cynthia H. Whaley, Henrik Skov, Martine Collaud Coen, Joakim Langner, Stephen R. Arnold
Writing – review & editing: Kathy S. Law, Jens L. Hjorth, Jakob B. Pernov, Cynthia H. Whaley, Henrik Skov, Martine Collaud Coen, Joakim Langner, Stephen R. Arnold, David Tarasick, Jesper Christensen, Peter Effertz, Michael Gauss, Ulas Im, Naga Oshima, Irina Petropavlovskikh, David Plummer, Svetlana Tsyro, Steven T. Turnock

production of anthropogenic or natural emissions of O_3 precursors, including nitrogen oxides (NO_x), carbon monoxide (CO) and methane (CH_4), in the Arctic, or following air mass transport from mid-latitudes, as well as transport of O_3 from the stratosphere (Law et al., 2014; Schmale et al., 2018). Sinks include photochemical destruction, including reactions involving halogens leading to so-called ozone depletion events (ODEs) (Barrie, et al., 1988; Simpson et al., 2007), and surface dry deposition (Clifton et al., 2020). Growth in anthropogenic emissions since pre-industrial times has led to increases in tropospheric O_3 throughout the Northern Hemisphere (NH) (Cooper et al., 2020; Gaudel et al., 2018; Tarasick et al., 2019; Turnock et al., 2020) contributing to observed global and Arctic warming over the past century (e.g., Griffiths et al., 2021; Szopa et al., 2021). Since the mid-1990s, a mix of relatively weak positive and negative trends (+1 to −1 parts per billion by volume (ppbv) per decade) have been reported in the NH at the surface and in the free troposphere (FT), with largest increases over south and eastern Asia, associated with increasing anthropogenic emissions (Cooper et al., 2020; H. Wang et al., 2022).

To date, only a few studies have focused on assessing tropospheric O_3 trends in the Arctic. While positive O_3 trends were diagnosed at several surface sites, results do not always have high certainty, and both positive and negative trends were reported at some Canadian sites (Cooper et al., 2020; Sharma et al., 2019; Tarasick et al., 2016). In the Arctic FT, studies found significant positive trends (B. Christiansen et al., 2017; H. Wang et al., 2022), no trends (Tarasick et al., 2016), or mixed trends in different seasons (Bahramvash Shams et al., 2019). Differences in the periods analyzed, sign or magnitude of trends, based on different methodologies, data averaging, etc. emphasizes the need to further examine trends using the same methodology. Coherent estimation of observed trends, and evaluation of modeled trends, is needed to better understand O_3 changes and impacts on Arctic climate that are sensitive to the altitude where O_3 perturbations occur (Rap et al., 2015). This study assesses annual/decadal and monthly trends, together with possible evolution in seasonal cycles, of Arctic tropospheric O_3 over the last 20–30 years. Observed changes are also compared to results from atmospheric chemistry-climate models run as part of the recent Arctic Monitoring and Assessment Programme (AMAP) SLCF assessment (AMAP, 2021; Whaley et al., 2022; von Salzen et al., 2022), taking into account reported model deficiencies (Whaley et al., 2023). Results are discussed in light of possible changes in sources and sinks of Arctic tropospheric O_3.

2. Methods

2.1. Measurements

The location of surface and ozonesonde sites used in this study are displayed in Figure 1, together with the Arctic Circle at 66.6°N, used to define the Arctic. Decadal surface trends are shown in the table grouped into (a) high Arctic coastal sites (Alert, Utqiaġvik/Barrow, Villum), Zeppelin (situated at 474 m on Svalbard) and Summit (high altitude (FT) site on Greenland (3,211 m)) and (b) European continental sites within (Pallas, Esrange), and just south (Tustervatn) of, the Arctic Circle.

Surface observations are from EBAS Level 2 data, station owners for Villum before 2001, Canada's Open Government Portal for Alert, and National Oceanic and Atmospheric Administration (NOAA) for Summit, and Barrow Atmospheric Observatory, Utqiaġvik (Utqiaġvik from now on). Ozonesonde data are from the World Ozone and Ultraviolet Radiation Data Center (WOUDC) and Network for the Detection of Atmospheric Composition Change (NDACC). See also Text S1, Figures S1 and S2 in Supporting Information S1, including data coverage.

2.2. Trend Analysis

Observed monthly and annual/decadal trends in surface O_3 concentrations at different sites are determined using a non-parametric Mann-Kendall method based on the 90th and 95th confidence limits (CLs) and Sen's slope methodology (Sen, 1968; Theil, 1950) and p-values (probability that trends occurred by chance). Daily median data are sorted into different months and pre-whitened, due to the presence of autocorrelation, via the 3PW algorithm from Collaud Coen et al. (2020). Trends using ozonesonde profiles are calculated based on weekly medians for selected pressure levels. See Text S2 in Supporting Information S1 for details and justification for use of our methods. We focus on discussing trends with high (95% CL, $p \leq 0.05$) and medium certainty (90% CL, $0.05 < p \leq 0.1$). CLs are shown in the Figures and p-values are given in Figure 1 and Tables S2–S5 in Supporting Information S1.

Site	Trend (ppbv/10 years)	p-value	Period
High Arctic:			
Alert	**0.94**	0.044	1999-2019
	0.79	0.038	1993-2019
Utqiagvik	1.51	0.129	1999-2019
	0.75	0.258	1993-2019
Villum	**3.24**	0.034	1999-2019
	1.13	0.162	1996-2019
Zeppelin	-0.36	0.497	1999-2019
	0.62	0.089	1993-2019
Summit	-1.28	0.142	2001-2019
European continental Arctic and near-Arctic:			
Esrange	0.24	0.697	1999-2019
	0.27	0.610	1993-2019
Pallas	-0.98	0.327	1999-2019
	-1.33	0.067	1995-2019
Tustervatn	**-1.79**	0.003	1999-2019
	-0.63	0.102	1994-2019

Figure 1. Left: Location of surface (bold) and ozonesonde (italic) sites and showing the Arctic Circle (66.55°N). Right: O$_3$ trends at surface sites in ppbv per decade and *p*-values. Trends (>90% confidence limit, $p \leq 0.1$) are in bold. Geographical coordinates for all sites are provided in Whaley et al. (2023). See text for details.

2.3. Modeled Trends

Modeled trends at the surface and different altitudes are calculated for 1995–2015 using results from four global chemistry-climate models (CMAM, GISS-E2.1, MRI-ESM2, UKESM1) and two chemistry-transport models (DEHM, EMEP MSC-W) run using the same ECLIPSEv6b anthropogenic emissions, and nudged with meteorological reanalyses as part of AMAP (2021). Details can be found in Whaley et al. (2022), Text S3 and Table S1 in Supporting Information S1. Simulated monthly mean O$_3$ volume mixing ratios from the model grid box containing the measurement location are used to compute multi-model medians (MMMs). For ozonesonde comparisons, modeled vertical profiles are interpolated onto the same vertical bins as the measurements before trends are computed.

3. Surface Ozone Trends in the Arctic

3.1. Observed Ozone Trends

Annual and decadal trends are calculated for 1993–2019, or for the longest period with sufficient data, for all the sites (see Figure 1, Table S2 in Supporting Information S1).

Average O$_3$ seasonal cycles are also calculated for earlier (1993–2000) and later (2012–2019) periods, to examine possible changes, together with monthly trends (Figure 2, Table S3 in Supporting Information S1 for *p*-values) at selected sites (see Figure S3 in Supporting Information S1 for other sites). Monthly trends are also analyzed for different 21-year periods (1993–2013, 1999–2019) (Figure S4 in Supporting Information S1).

First considering high Arctic sites at coastal locations that exhibit a winter maximum with low spring concentrations attributed to ODEs, as discussed in Whaley et al. (2023). Alert has positive O$_3$ annual trends ($p = 0.044$), as does Villum ($p = 0.034$) for the shorter time period 1999–2019, while annual trends at Utqiaġvik are not apparent (see Figure 1/Table S2 in Supporting Information S1). Trends are also calculated in particular seasons, as shown in Figure 2. Notably, positive trends are found during late autumn and/or winter at Alert, Villum and Utqiaġvik (p's ≤ 0.022). Positive trends are also calculated in spring (April-May) and August at Utqiaġvik. Winter trends at Alert and spring trends at Utqiaġvik are more pronounced over the later record (1999–2019) (see Figure S4
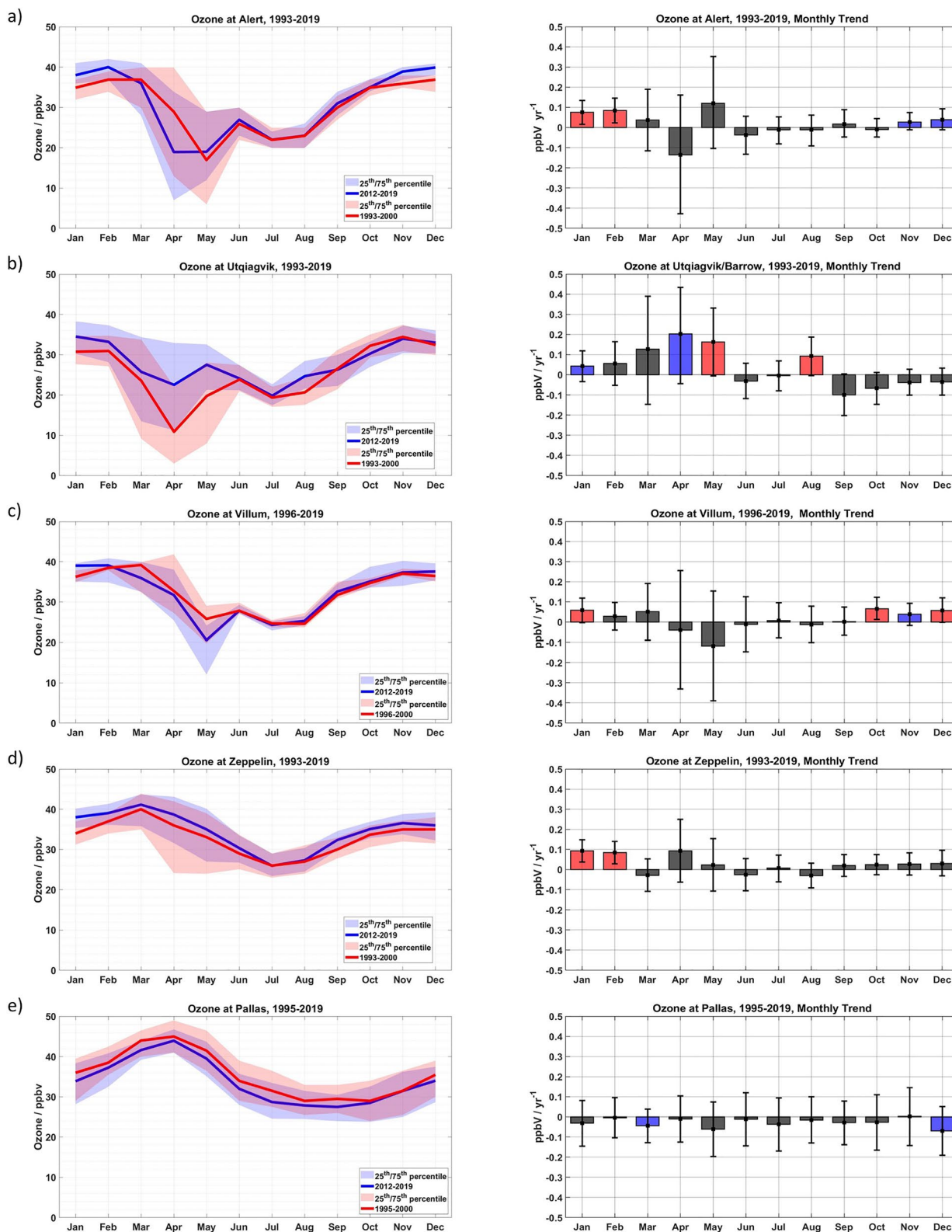
Figure 2. Observed surface O$_3$ trends and seasonal cycles. Left: seasonal cycles of monthly median O$_3$ (ppbv) at (a) Alert, (b) Utqiaġvik, (c) Villum, (d) Zeppelin, and (e) Pallas for 1993–2000 (red lines) versus 2012–2019 (blue lines). Shaded areas show upper and lower quartiles of hourly values. Right: monthly trends for 1993–2019. Boxes represent the slope of the trend in ppbv per year with red boxes having 95th% confidence limit (CL), blue boxes 90th% CL, and black boxes are trends with low certainty. Error bars show 95% CLs. Results are shown for shorter periods depending on data availability.

in Supporting Information S1). To further characterize these changes, probability distributions in observed O_3 concentrations are calculated for periods with at least 90% CL monthly trends (see Figure S5 in Supporting Information S1). Positive trends during winter and spring at Utqiaġvik are the result of a decrease (increase) in the frequency of low (high) concentrations (January–May), whereas wintertime O_3 concentrations shifted recently towards higher values at Alert (November–February) and Villum (October–January). Zeppelin shows a different seasonal behavior compared to Arctic sea-level coastal sites with a spring maximum, more similar to remote mid-latitude sites. Here, positive annual trends are estimated for 1993–2019 (Figure 1, $p = 0.089$), and in Jan./Feb. (Figure 2, $p \leq 0.001$), driven by increases in the earlier part of the record (1993–2013) (Figure S4 in Supporting Information S1).

Continental northern Scandinavian sites exhibit a different behavior with Tustervatn ($p = 0.003$), and Pallas, with lower certainty ($p = 0.067$), showing negative annual trends but no clear annual (or monthly) trends at Esrange ($p > 0.151$) over any of the periods considered. The shape of the seasonal cycle for the earlier versus the later period is similar at these sites, which also have a spring maximum like Zeppelin. O_3 appears to be decreasing throughout the year when comparing earlier and later periods although negative trends are only evident at Pallas (March, December), and at Tustervatn in spring and early summer for 1999–2019 trends (Figure S4 in Supporting Information S1). Summit is more representative of the FT and samples air masses transported from North America and Asia, or of stratospheric origin (Dibb, 2007; Schmeisser et al., 2018). No clear annual trend, calculated over the shorter 2001–2019 record, is seen, but negative monthly trends are estimated for January, March-May and September ($p \leq 0.060$).

3.2. Comparison of Observed and Modeled Surface Trends

Figure 3 compares observed monthly and MMM trends for 1995–2015, or the closest possible time interval in case of years with missing observations. Results for other sites are shown in Figure S6 of Supporting Information S1 and p-values in Table S4 of Supporting Information S1. Observed trends are more frequently diagnosed over 1993–2019 (Figure 2) than over the shorter period ending in 2015 (Figure 3). While the MMMs simulate O_3 seasonal cycles reasonably well, low O_3 concentrations are missed in spring, and wintertime O_3 is underestimated (Whaley et al., 2023). The MMMs simulate positive trends at Zeppelin (Jan., $p = 0.048$) and negative trends at Esrange (May, $p = 0.017$), respectively, but not observed positive trends at Utqiaġvik (April, $p = 0.035$). Trends are simulated, but not observed, at Alert (January, December, $p = 0.058, 0.014$), Zeppelin (April, $p = 0.032$), Villum (Sept., $p = 0.035$), and Tustervatn (March, $p = 0.057$).

4. Arctic Ozone Trends in the Free Troposphere

4.1. Observed Vertical Trends

This analysis focuses on O_3 changes in the lower and mid-troposphere. Figure 4 shows observed relative trends at six Arctic ozonesonde sites from 925 to 400 hPa for 1993–2019 (see p-values in Table S5 of Supporting Information S1). Absolute trends above and below 400 hPa, and relative trends from 925 to 100 hPa, providing information on changes in the upper troposphere (UT) and lower stratosphere (LS), are also calculated (Figures S7a and S7b in Supporting Information S1). Overall, while there are few high confidence trends, there seems to be a "dipole effect" with positive trends in winter and summer, and negative trends in spring and autumn. Positive winter (notably Jan.) trends are found up to 400 hPa at most sites (except Resolute and Sodankyla), and at Scoresbysund in early spring. Positive wintertime trends are more evident in the earlier period in the UTLS (Figure S8 in Supporting Information S1). Eureka, Resolute, and Sodankyla have periods with negative trends especially during spring and early summer in the lower troposphere (LT). Resolute decreases extend up to 500 hPa in March-April. Relative trends vary from −1.5% to +0.5–1.0% per year (Figure 4 and Figure S7b in Supporting Information S1) while stronger negative trends are diagnosed in later years (1999–2019) compared to 1993–2013 at all sites (Figure S8 in Supporting Information S1).

4.2. Comparison of Observed and Modeled Vertical Trends

Figure 5 shows observed ozonesonde and MMM trends for 1995–2015 up to 400 hPa (see Figure S9 in Supporting Information S1 for results up to 100 hPa). Only results from five models are used, since EMEP MSC-W only
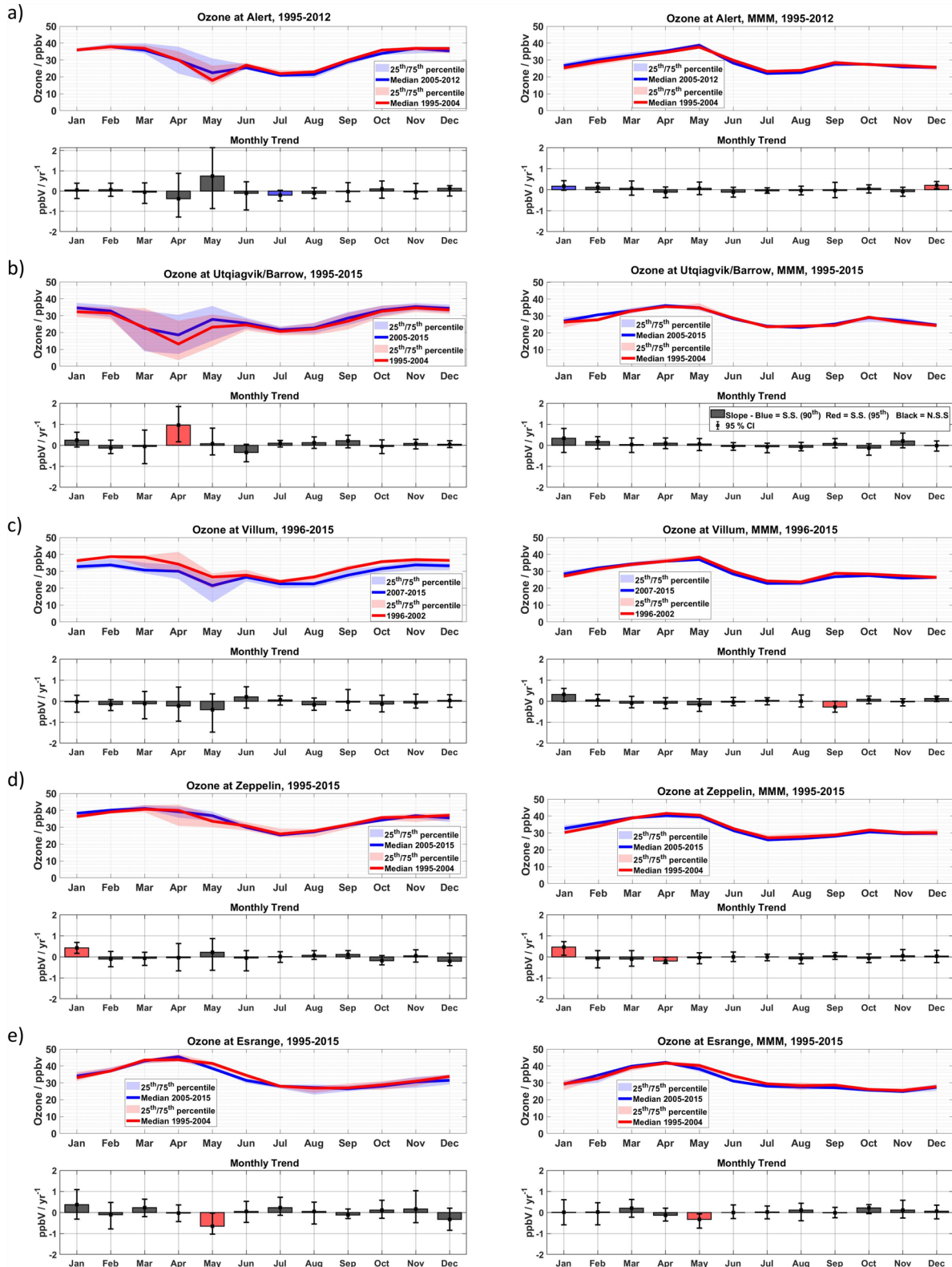
Figure 3. Comparison of observed (left) and multi-model median (right) surface O_3 trends and seasonal cycles at (a) Alert, (b) Utqiaġvik, (c) Villum, (d) Zeppelin, and (e) Esrange. Upper panels: seasonal cycles for 1995–2004 (red lines) versus 2005–2015 (blue lines). Shaded areas show upper and lower quartiles of monthly values (observations only). Lower panels: monthly median trends in ppbv per year for 1995–2015, or shorter periods depending on data availability. Box coloring and error bars same as Figure 2.
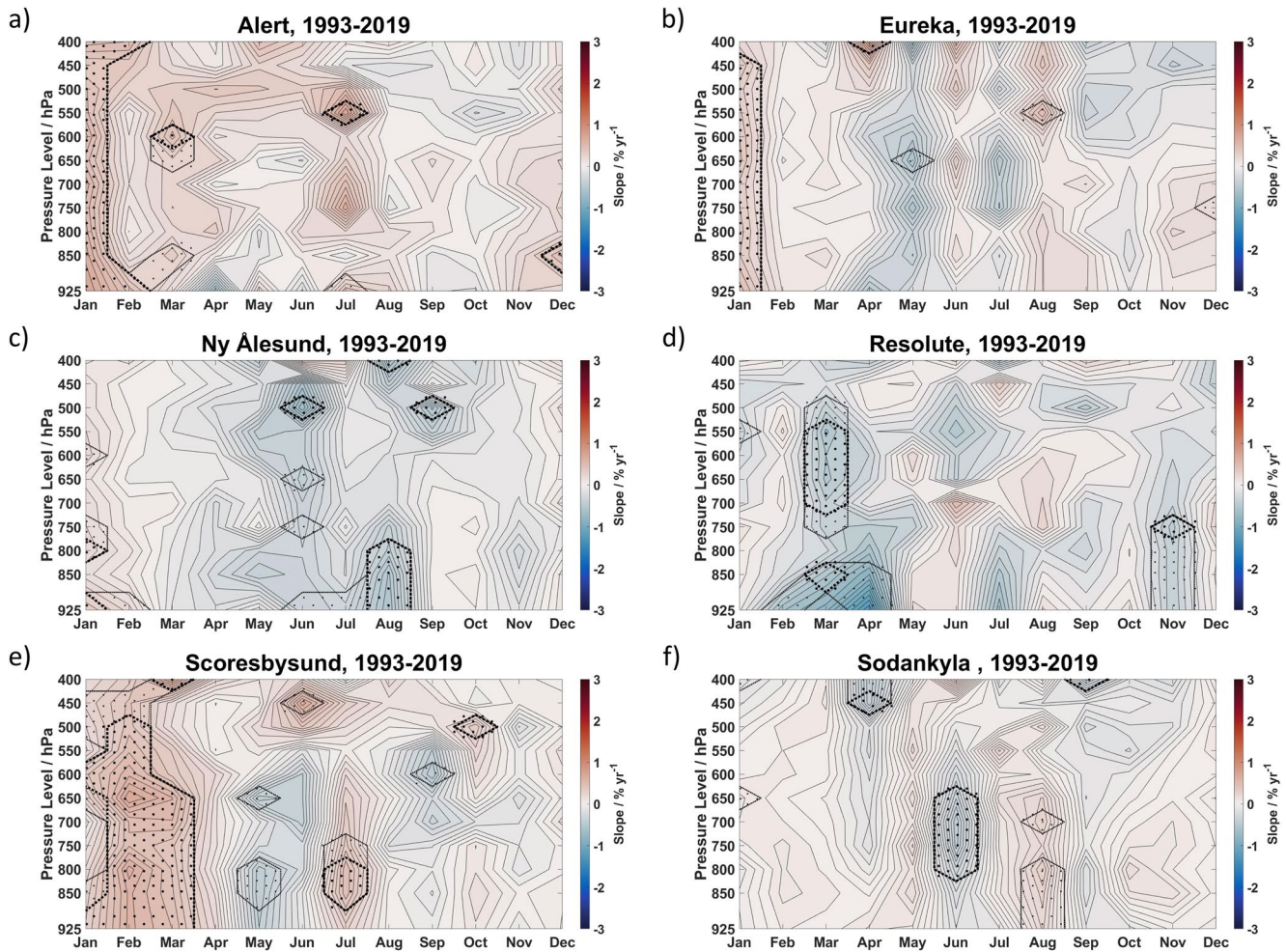
Figure 4. Vertical trends in observed monthly O$_3$ for 1993–2019, relative to monthly median concentrations, in % per year, from 925 to 400 hPa at (a) Alert, (b) Eureka, (c) Ny Ålesund, (d) Resolute, (e) Scoresbysund, and (f) Sodankyla. Stippled lines/areas show trends having 90th% confidence limit (CL) (smaller marker size) and 95th % CL (larger marker size).

provided surface O$_3$. The MMMs appear to capture the observed "dipole effect" seen in the observed trends. Models also capture observed increases in the winter but trends are overestimated at most sites, especially at Ny Ålesund. Negative winter trends at Resolute are not simulated. This may be linked to positive modeled winter trends above 500 hPa at all sites (see also Figure S9 in Supporting Information S1). Summertime positive MMM trends are larger than observed trends at some sites, for example, Resolute and Ny Ålesund.

5. Discussion and Conclusions

Increasing annual surface O$_3$ trends at Arctic coastal sites, and at Zeppelin, are in qualitative agreement with Cooper et al. (2020), but in contrast to negative or non-significant surface trends at Canadian sites (Tarasick et al., 2016). A notable finding is that positive trends occur mainly in the winter months. While such increases were reported previously at Utqiaġvik (A. Christiansen et al., 2022; Cooper et al., 2020) and Alert (Sharma et al., 2019), we confirm this tendency over the wider Arctic. Emission reductions of NO$_x$ in Europe and North America, and more recently over eastern Asia, have led to increasing wintertime O$_3$ at mid-latitudes due to less nitrogen oxide titration of O$_3$ (Bowman et al., 2022; Jhun et al., 2015; T. Wang et al., 2022). This can explain observed increases in wintertime surface Arctic O$_3$, influenced primarily by transport of air masses from Europe (Hirdman et al., 2010). Evidence for declining O$_3$ precursor trends is supported by decreases in observed CO in the Arctic during autumn and winter (Figure S10 in Supporting Information S1). At the same time, CH$_4$ continues to increase globally contributing to rising O$_3$ in the NH (Zeng et al., 2022) (see also Text S4 in Supporting Information S1 on Arctic O$_3$ precursor trends).
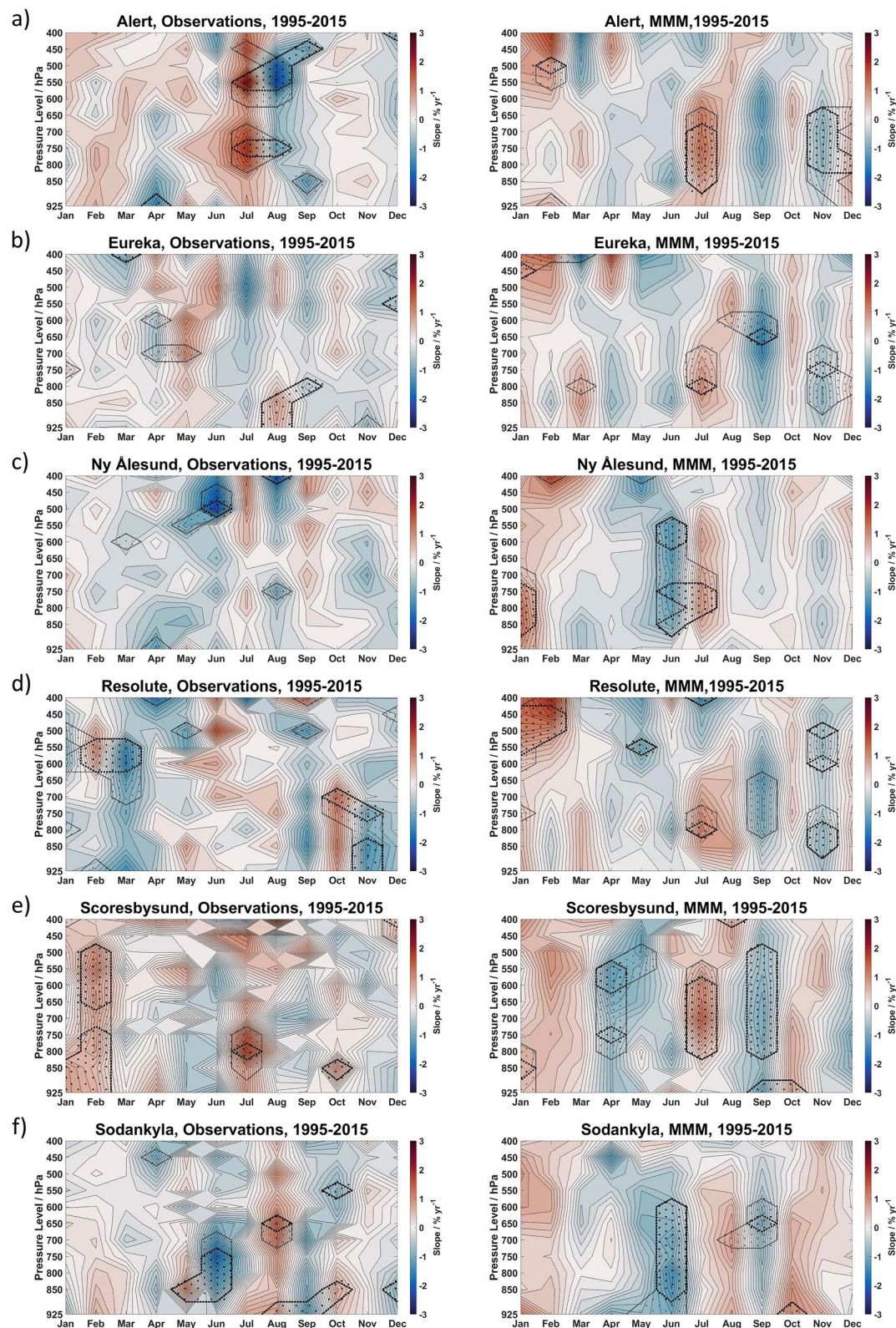
Figure 5. Comparison of observed (left) and multi-model median (right) vertical trends in monthly O_3, relative to monthly medians, in % per year, from 925 to 400 hPa over 1995–2015 at (a) Alert, (b) Eureka, (c) Ny Ålesund, (d) Resolute, (e) Scoresbysund, and (f) Sodankyla. Shading/symbols are as in Figure 4.

Another intriguing finding is springtime surface O_3 increases at Utqiaġvik (especially over 1999–2019, Figure S4 in Supporting Information S1), but no discernible trends at Alert and Villum. Changes in O_3 concentrations at this time of year may be driven by changes in ODE frequency linked to climate change or weather patterns (Oltmans et al., 2012). ODEs lead to zero or very low springtime O_3 due to bromine released from frost flowers or blowing snow (on sea-ice) (Simpson et al., 2007; Yang et al., 2008, 2010) or iodine compounds with a possible oceanic source (Benavent et al., 2022). Increasing prevalence of first year sea-ice leading to increasing sea-spray aerosols from blowing snow (Confer et al., 2023) may explain increases in springtime tropospheric bromine oxide, observed from satellites, along the north coast of Greenland and central Arctic Ocean (Bougoudis et al., 2020). Indeed, the frequency of low springtime O_3 concentrations has been increasing at Canadian high Arctic sites (see Figure S11 in Supporting Information S1) but no clear springtime monthly trends are determined at Alert or Villum in our analysis. Springtime increases at Utqiaġvik could be due to stronger transport from mid-latitudes to this site during periods with a more northerly extension of the Pacific storm track, hampering conditions for ODEs (Koo et al., 2012). They could also be due to an increasing influence from local emissions, such as shipping or Alaskan petroleum extraction, when photochemistry becomes active in spring (Gunsch et al., 2017).

Decreases in springtime/early summer O_3 in northern Scandinavia, especially over the later 1999–2019 period, are consistent with negative trends reported at Tustervatn since 1995 (Cooper et al., 2020), and in northern Sweden during summer (Andersson et al., 2017). These decreases are associated with lower maximum O_3 concentrations linked to reductions in European precursor emissions leading to less photochemical O_3 production (Cooper et al., 2020) although no clear trends in observed springtime CO are found at Zeppelin (Figure S10 in Supporting Information S1). Springtime negative trends at Summit may also be due to emission reductions over North America. Our results do not suggest a shift in the O_3 seasonal cycle toward higher concentrations in the spring (i.e., moving back toward pre-industrial O_3 seasonality) as reported at NH mid-latitudes (Bowman et al., 2022). Another explanation for decreasing springtime O_3 at the surface could be that reductions in snow cover due to climate warming (Mudryk et al., 2020) are leading to more O_3 dry deposition to Scandinavian forests.

The observed and modeled surface trend comparison covers 1995–2015, thereby missing the later time period when stronger observed O_3 trends are found, especially positive trends in winter. MMMs capture wintertime O_3 increases at Zeppelin, but overestimate at Alert although they simulate decreasing surface winter CO at Alert and Utqiaġvik (Figure S10 in Supporting Information S1). This suggests that while anthropogenic emission changes may be captured, other model deficiencies may be contributing, such as modeling shallow boundary layers, O_3 deposition or NO_x lifetimes, as noted by Whaley et al. (2023). The MMMs miss springtime increases at Utqiaġvik. This could be due to incorrect simulation of transport patterns (Oltmans et al., 2012) or missing surface halogen chemistry leading to incorrect modeled seasonality (Whaley et al., 2023). Negative springtime (May) Scandinavian trends are not always reproduced, possibly reflecting issues in the emission trends or modeled dry deposition.

Positive FT O_3 trends in winter at most Arctic sites are found, in common with several coastal Arctic surface sites, and in-line with increases reported at NH mid-latitudes (Gaudel et al., 2018), and at Canadian ozonesonde sites, except Resolute (H. Wang et al., 2022). Patterns in observed trends are quite well captured by the MMMs over 1995–2015, notably positive trends in winter and summer, although they tend to be overestimated. Positive summer trends may be linked to increased photochemical production from increased lightning and boreal fires due to climate warming (Veraverbeke et al., 2017). Observed negative trends in spring, extending from near the surface into the FT, are generally reproduced, and are likely to be due to decreasing NO_x emissions leading to lower FT O_3 where photochemical production is NO_x-limited. Negative LT trends could also be due to increasing ODEs extending over 100 kms and up to 1.5 km (Yang et al., 2020; Zilker et al., 2023). Overestimation of winter trends contrasts to previous studies where models underestimated NH trends (A. Christiansen et al., 2022; H. Wang et al., 2022). This may be due to differences in model transport or O_3 precursor emission trends, including NO_x reductions (see also Text S4 in Supporting Information S1). AMAP models overestimate mid-latitude FT O_3 (Whaley et al., 2023), possibly suggesting a larger sensitivity to precursor emission changes.

Observed trends in the UT (LS) appear to have switched from positive to negative since 1993 in winter/spring, which may explain stronger positive FT trends in the earlier part of the record (1993–2013). More frequent positive phases of the Arctic Oscillation in recent years may be contributing with a weaker Brewer-Dobson circulation leading to less transport of stratospheric O_3 into the Arctic UTLS, a higher tropopause height, and thus lower O_3 concentrations in this region (Zhang et al., 2017). However, Liu et al. (2020) did not detect any trend in the

stratospheric O_3 flux into the Arctic UT. On the other hand, H. Wang et al. (2022) attributed FT increases in NH mid-high latitude O_3 to increases in aircraft NO_x emissions.

Overall, this study identifies trends with high-medium certainty in observed Arctic tropospheric O_3 that are generally quite well captured by MMM results, Further investigation into the causes of observed trends, and model performance, are needed taking into account uncertainties in the observations and models (Fiore et al., 2022; Young et al., 2018), including known model issues (Whaley et al., 2023).

Conflict of Interest

The authors declare no conflicts of interest relevant to this study.

Data Availability Statement

Surface O_3 monitoring datasets are provided by EMEP (European Monitoring and Evaluation Program), and Global Atmosphere Watch (GAW) World Data Centre for Reactive Gases. EMEP and GAW O_3 data are available via the EBAS data portal (from end of 1989 to present). CO data at Utqiaġvik/Barrow and Zeppelin are also available via the EBAS data portal: http://ebas.nilu.no. Select the station name, and the component (CO, O_3) to access the data files. Canadian surface O_3 data can be downloaded from: https://data-donnees.ec.gc.ca/data/air/monitor/networks-and-studies/alert-nunavut-ground-level-ozone-study/. Canadian surface CO is available at: https://data-donnees.ec.gc.ca/data/air/monitor/national-air-pollution-surveillance-naps-program/?lang=en. Click on folders Data, Year, ContinuousData, then HourlyData. Surface O_3 records for Utqiaġvik/Barrow (BRW) and Summit (SUM) are provided by P. Effertz and I. Petropavlovskikh via NOAA GML. Data is available at https://gml.noaa.gov/aftp/data/ozwv/SurfaceOzone/. Click on the directories for BRM or SUM to obtain the data. Surface O_3 measurements at Summit are made possible via the U.S. National Science Foundation Office of Polar Programs and their contract with Battelle Arctic Research Operations (contract #49100420C0001). Ny Ålesund, Scoresbysund and Sodankylä ozonesonde data are obtained as part of the NDACC. Data is available via https://ndacc.larc.nasa.gov/index.php/stations. Click on the relevant site location to access the data files. Ozonesonde data for Alert, Resolute and Eureka have been reprocessed according to Tarasick et al. (2016), available at https://hegiftom.meteo.be/datasets/ozonesondes.

All model output files in NetCDF format from the simulations used in this study can be found here: https://open.canada.ca/data/en/dataset/c9a333ea-b81c-4df3-9880-ea7c3daeb76f. Model codes for GISS-E2.1 are available at: https://www.giss.nasa.gov/tools/modelE/.

Open-source codes for the Mann-Kendall test associated with Sen's slope are distributed under the BSD 3-Clause Licence in dedicated GitHub repositories hosted within the "mannkendall" directory (https://github.com/mannkendall): Matlab (Collaud Coen & Vogt, 2020, https://doi.org/10.5281/zenodo.4134618, https://github.com/mannkendall/Matlab), Python (Vogt, 2020, https://doi.org/10.5281/zenodo.4134435, https://github.com/mannkendall/Python), and R (Bigi & Vogt, 2020, https://doi.org/10.5281/zenodo.4134632, https://github.com/mannkendall/R). Last access for all codes 27 January 2023.

References

AMAP. (2015). *AMAP Assessment 2015: Black carbon and ozone as Arctic climate forcers* (Vol. 116). Arctic Monitoring and Assessment Programme (AMAP). Retrieved from https://www.amap.no/documents/doc/amap-assessment-2015-black-carbon-and-ozone-as-arctic-climate-forcers/1299

AMAP. (2021). *AMAP Assessment 2021: Impacts of short-lived climate forcers on Arctic climate, air quality, and human health*. Arctic Monitoring and Assessment Programme (AMAP). Retrieved from https://www.amap.no/documents/doc/amap-assessment-2021-impacts-of-short-lived-climate-forcers-on-arctic-climate-air-quality-and-human-health/3614

Andersson, C., Alpfjord, H., Robertson, L., Karlsson, P. E., & Engardt, M. (2017). Reanalysis of and attribution to near-surface ozone concentrations in Sweden during 1990–2013. *Atmospheric Chemistry and Physics*, *17*(22), 13869–13890. https://doi.org/10.5194/acp-17-13869-2017

Anenberg, S. C., Horowitz, L. W., Tong, D. Q., & West, J. J. (2010). An estimate of the global burden of anthropogenic ozone and fine particulate matter on premature human mortality using atmospheric modeling. *Environmental Health Perspectives*, *118*(9), 1189–1195. https://doi.org/10.1289/ehp.0901220

Arnold, S. R., Lombardozzi, D., Lamarque, J.-F., Richardson, T., Emmons, L. K., Tilmes, S., et al. (2018). Simulated global climate response to tropospheric ozone-induced changes in plant transpiration. *Geophysical Research Letters*, *45*(23), 13070–13079. https://doi.org/10.1029/2018GL079938

Bahramvash Shams, S., Walden, V. P., Petropavlovskikh, I., Tarasick, D., Kivi, R., Oltmans, S., et al. (2019). Variations in the vertical profile of ozone at four high-latitude Arctic sites from 2005 to 2017. *Atmospheric Chemistry and Physics*, *19*(15), 9733–9751. https://doi.org/10.5194/acp-19-9733-2019

Barrie, L., Bottenheim, J., Schnell, R., Crutzen, P. J., & Rasmussen, R. A. (1988). Ozone destruction and photochemical reactions at polar sunrise in the lower Arctic atmosphere. *Nature*, *334*(6178), 138–141. https://doi.org/10.1038/334138a0

Benavent, N., Mahajan, A. S., Li, Q., Cuevas, C. A., Schmale, J., Angot, H., et al. (2022). Substantial contribution of iodine to Arctic ozone destruction. *Nature Geoscience*, *15*(10), 770–773. https://doi.org/10.1038/s41561-022-01018-w

Bigi, A., & Vogt, F. P. A. (2020). mannkendall/R: First release, Version v1.0.0 [Dataset]. Zenodo. https://doi.org/10.5281/zenodo.4134632

Bougoudis, I., Blechschmidt, A.-M., Richter, A., Seo, S., Burrows, J. P., Theys, N., & Rinke, A. (2020). Long-term time series of Arctic tropospheric BrO derived from UV–VIS satellite remote sensing and its relation to first-year sea ice. *Atmospheric Chemistry and Physics*, *20*(20), 11869–11892. https://doi.org/10.5194/acp-20-11869-2020

Bowman, H., Turnock, S., Bauer, S. E., Tsigaridis, K., Deushi, M., Oshima, N., et al. (2022). Changes in anthropogenic precursor emissions drive shifts in the ozone seasonal cycle throughout the northern midlatitude troposphere. *Atmospheric Chemistry and Physics*, *22*(5), 3507–3524. https://doi.org/10.5194/acp-22-3507-2022

Christiansen, A., Mickley, L. J., Liu, J., Oman, L. D., & Hu, L. (2022). Multidecadal increases in global tropospheric ozone derived from ozonesonde and surface site observations: Can models reproduce ozone trends? *Atmospheric Chemistry and Physics*, *22*(22), 14751–14782. https://doi.org/10.5194/acp-22-14751-2022

Christiansen, B., Jepsen, N., Kivi, R., Hansen, G., Larsen, N., & Korsholm, U. S. (2017). Trends and annual cycles in soundings of Arctic tropospheric ozone. *Atmospheric Chemistry and Physics*, *17*(15), 9347–9364. https://doi.org/10.5194/acp-17-9347-2017

Clifton, O. E., Fiore, A. M., Massman, W. J., Baublitz, C. B., Coyle, M., Emberson, L., et al. (2020). Dry deposition of ozone over land: Processes, measurement, and modeling. *Reviews of Geophysics*, *58*(1), e2019RG000670. https://doi.org/10.1029/2019rg000670

Collaud Coen, M., Andrews, E., Bigi, A., Martucci, G., Romanens, G., Vogt, F. P. A., & Vuilleumier, L. (2020). Effects of the prewhitening method, the time granularity, and the time segmentation on the Mann–Kendall trend detection and the associated Sen's slope. *Atmospheric Measurement Techniques*, *13*(12), 6945–6964. https://doi.org/10.5194/amt-13-6945-2020

Collaud Coen, M., & Vogt, F. P. A. (2020). mannkendall/Matlab: First release, Version V1.0.0 [Dataset]. Zenodo. https://doi.org/10.5281/zenodo.4134618

Confer, K. L., Jaeglé, L., Giston, G. E., Sharma, S., Nandan, V., Yackel, J., et al. (2023). Impact of changing Arctic sea ice extent, sea ice age, and snow depth on sea salt aerosol from blowing snow and the open ocean for 1980–2017. *Journal of Geophysical Research: Atmospheres*, *128*, e2022JD037667. https://doi.org/10.1029/2022JD037667

Cooper, O. R., Schultz, M. G., Schröder, S., Chang, K.-L., Gaudel, A., Benítez, G. C., et al. (2020). Multi-decadal surface ozone trends at globally distributed remote locations. *Elementa: Science of the Anthropocene*, *8*, 23. https://doi.org/10.1525/elementa.420

Dibb, J. E. (2007). Vertical mixing above Summit, Greenland: Insights into seasonal and high frequency variability from the radionuclide tracers ^{7}Be and ^{210}Pb. *Atmospheric Environment*, *41*(24), 5020–5030. https://doi.org/10.1016/j.atmosenv.2006.12.005

Fiore, A. M., Hancock, S. E., Lamarque, J.-F., Correa, G. P., Chang, K.-L., Ru, M., et al. (2022). Understanding recent tropospheric ozone trends in the context of large internal variability: A new perspective from chemistry-climate model ensembles. *Environmental Research: Climate*, *1*(2), 025008. https://doi.org/10.1088/2752-5295/ac9cc2

Gaudel, A., Cooper, O. R., Ancellet, G., Barret, B., Boynard, A., Burrows, J. P., et al. (2018). Tropospheric Ozone Assessment Report: Present-day distribution and trends of tropospheric ozone relevant to climate and global atmospheric chemistry model evaluation. *Elementa: Science of the Anthropocene*, *6*, 39. https://doi.org/10.1525/elementa.291

Griffiths, P. T., Murray, L. T., Zeng, G., Shin, Y. M., Abraham, N. L., Archibald, A. T., et al. (2021). Tropospheric ozone in CMIP6 simulations. *Atmospheric Chemistry and Physics*, *21*(5), 4187–4218. https://doi.org/10.5194/acp-21-4187-2021

Gunsch, M. J., Kirpes, R. M., Kolesar, K. R., Barrett, T. E., China, S., Sheesley, R. J., et al. (2017). Contributions of transported Prudhoe Bay oil field emissions to the aerosol population in Utqiaġvik, Alaska. *Atmospheric Chemistry and Physics*, *17*(17), 10879–10892. https://doi.org/10.5194/acp-17-10879-2017

Hirdman, D., Sodemann, H., Eckhardt, S., Burkhart, J. F., Jefferson, A., Mefford, T., et al. (2010). Source identification of short-lived air pollutants in the Arctic using statistical analysis of measurement data and particle dispersion model output. *Atmospheric Chemistry and Physics*, *10*(2), 669–693. https://doi.org/10.5194/acp-10-669-2010

Jhun, I., Coull, B. A., Zanobetti, A., & Koutrakis, P. (2015). The impact of nitrogen oxides concentration decreases on ozone trends in the USA. *Air Quality, Atmosphere and Health*, *8*(3), 283–292. https://doi.org/10.1007/s11869-014-0279-2

Koo, J. H., Wang, Y., Kurosu, T. P., Chance, K., Rozanov, A., Richter, A., et al. (2012). Characteristics of tropospheric ozone depletion events in the Arctic spring: Analysis of the ARCTAS, ARCPAC, and ARCIONS measurements and satellite BrO observations. *Atmospheric Chemistry and Physics*, *12*(20), 9909–9922. https://doi.org/10.5194/acp-12-9909-2012

Law, K. S., Stohl, A., Quinn, P. K., Brock, C. A., Burkhart, J. F., Paris, J.-D., et al. (2014). Arctic air pollution: New insights from POLARCAT-IPY. *Bulletin of the American Meteorological Society*, *95*(12), 1873–1895. https://doi.org/10.1175/bams-d-13-00017.1

Liu, J., Rodriguez, J. M., Oman, L. D., Douglass, A. R., Olsen, M. A., & Hu, L. (2020). Stratospheric impact on the Northern Hemisphere winter and spring ozone interannual variability in the troposphere. *Atmospheric Chemistry and Physics*, *20*(11), 6417–6433. https://doi.org/10.5194/acp-20-6417-2020

Mudryk, L., Santolaria-Otín, M., Krinner, G., Ménégoz, M., Derksen, C., Brutel-Vuilmet, C., et al. (2020). Historical Northern Hemisphere snow cover trends and projected changes in the CMIP6 multi-model ensemble. *The Cryosphere*, *14*(7), 2495–2514. https://doi.org/10.5194/tc-14-2495-2020

Oltmans, S. J., Johnson, B. J., & Harris, J. M. (2012). Springtime boundary layer ozone depletion at Barrow, Alaska: Meteorological influence, year-to-year variation, and long-term change. *Journal of Geophysical Research*, *117*(D14), D00R18. https://doi.org/10.1029/2011JD016889

Rap, A., Richards, N. A. D., Forster, P. M., Monks, S. A., Arnold, S. R., & Chipperfield, M. P. (2015). Satellite constraint on the tropospheric ozone radiative effect. *Geophysical Research Letters*, *42*(12), 5074–5081. https://doi.org/10.1002/2015GL064037

Sand, M., Berntsen, T. K., von Salzen, K., Flanner, M. G., Langner, J., & Victor, D. G. (2016). Response of Arctic temperature to changes in emissions of short-lived climate forcers. *Nature Climate Change*, *6*(3), 286–289. https://doi.org/10.1038/nclimate2880

Schmale, J., Arnold, S. R., Law, K. S., Thorp, T., Anenberg, S., Simpson, W. R., et al. (2018). Local Arctic air pollution: A neglected but serious problem. *Earth's Future*, *6*(10), 1385–1412. https://doi.org/10.1029/2018ef000952

Schmeisser, L., Backman, J., Ogren, J. A., Andrews, E., Asmi, E., Starkweather, S., et al. (2018). Seasonality of aerosol optical properties in the Arctic. *Atmospheric Chemistry and Physics*, *18*(16), 11599–11622. https://doi.org/10.5194/acp-18-11599-2018

Sen, P. K. (1968). Estimates of the regression coefficient based on Kendall's Tau. *Journal of the American Statistical Association*, *63*(324), 1379–1389. https://doi.org/10.1080/01621459.1968.10480934

Sharma, S., Barrie, L. A., Magnusson, E., Brattstrom, G., Leaitch, W. R., Steffen, A., & Landsberger, S. (2019). A factor and trends analysis of multidecadal lower tropospheric observations of Arctic aerosol composition, black carbon, ozone, and Mercury at Alert, Canada. *Journal of Geophysical Research-Atmospheres*, *124*(24), 14133–14161. https://doi.org/10.1029/2019JD030844

Simpson, W. R., von Glasow, R., Riedel, K., Anderson, P., Ariya, P., Bottenheim, J., et al. (2007). Halogens and their role in polar boundary-layer ozone depletion. *Atmospheric Chemistry and Physics*, *7*(16), 4375–4418. https://doi.org/10.5194/acp-7-4375-2007

Szopa, S., Naik, V., Adhikary, B., Artaxo, P., Berntsen, T., Collins, W. D., et al. (2021). Short-lived climate forcers. In *Climate Change 2021: The Physical Science Basis. Contribution of Working Group I to the Sixth Assessment Report of the Intergovernmental Panel on Climate Change* (pp. 817–922). Cambridge University Press. https://doi.org/10.1017/9781009157896.008

Tarasick, D., Galbally, I. E., Cooper, O. R., Schultz, M. G., Ancellet, G., Leblanc, T., et al. (2019). Tropospheric Ozone Assessment Report: Tropospheric ozone from 1877 to 2016, observed levels, trends and uncertainties. *Elementa: Science of the Anthropocene*, *7*, 39. https://doi.org/10.1525/elementa.376

Tarasick, D. W., Davies, J., Smit, H. G. J., & Oltmans, S. J. (2016). A re-evaluated Canadian ozonesonde record: Measurements of the vertical distribution of ozone over Canada from 1966 to 2013. *Atmospheric Measurement Techniques*, *9*(1), 195–214. https://doi.org/10.5194/amt-9-195-2016

Theil, H. (1950). A rank-invariant method of linear and polynomial regression analysis. *Proceedings, Koninklijke Nederlandse Akademie van Wetenschappen*, *53*, 386–392.

Turnock, S. T., Allen, R. J., Andrews, M., Bauer, S. E., Deushi, M., Emmons, L., et al. (2020). Historical and future changes in air pollutants from CMIP6 models. *Atmospheric Chemistry and Physics*, *20*(23), 14547–14579. https://doi.org/10.5194/acp-20-14547-2020

Veraverbeke, S., Rogers, B., Goulden, M., Jandt, R. R., Miller, C. E., Wiggins, E. B., & Randerson, J. T. (2017). Lightning as a major driver of recent large fire years in North American boreal forests. *Nature Climate Change*, *7*, 529–534. https://doi.org/10.1038/nclimate3329

Vogt, F. P. A. (2020). mannkendall/Python: First release, Version v1.0.0 [Dataset]. Zenodo. https://doi.org/10.5281/zenodo.4134435

von Salzen, K., Whaley, C. H., Anenberg, S. C., Van Dingenen, R., Klimont, Z., Flanner, M. G., et al. (2022). Clean air policies are key for successfully mitigating Arctic warming. *Communications Earth & Environment*, *3*(1), 222. https://doi.org/10.1038/s43247-022-00555-x

Wang, H., Lu, X., Jacob, D. J., Cooper, O. R., Chang, K.-L., Li, K., et al. (2022). Global tropospheric ozone trends, attributions, and radiative impacts in 1995–2017: An integrated analysis using aircraft (IAGOS) observations, ozonesonde, and multi-decadal chemical model simulations. *Atmospheric Chemistry and Physics*, *22*(20), 13753–13782. https://doi.org/10.5194/acp-22-13753-2022

Wang, T., Xue, L., Feng, Z., Dai, J., Zhang, Y., & Tan, Y. (2022). Ground-level ozone pollution in China: A synthesis of recent findings on influencing factors and impacts. *Environmental Research Letters*, *17*(6), 063003. https://doi.org/10.1088/1748-9326/ac69fe

Whaley, C. H., Law, K. S., Hjorth, J. L., Skov, H., Arnold, S. R., Langner, J., et al. (2023). Arctic tropospheric ozone: Assessment of current knowledge and model performance. *Atmospheric Chemistry and Physics*, *23*(1), 637–661. https://doi.org/10.5194/acp-23-637-2023

Whaley, C. H., Mahmood, R., von Salzen, K., Winter, B., Eckhardt, S., Arnold, S., et al. (2022). Model evaluation of short-lived climate forcers for the Arctic Monitoring and Assessment Programme: A multi-species, multi-model study. *Atmospheric Chemistry and Physics*, *22*(9), 5775–5828. https://doi.org/10.5194/acp-22-5775-2022

Yang, X., Blechschmidt, A.-M., Bognar, K., McClure-Begley, A., Morris, S., Petropavlovskikh, I., et al. (2020). Pan-Arctic surface ozone: Modelling vs. measurements. *Atmospheric Chemistry and Physics*, *20*(24), 15937–15967. https://doi.org/10.5194/acp-20-15937-2020

Yang, X., Pyle, J. A., & Cox, R. A. (2008). Sea salt aerosol production and bromine release: Role of snow on sea ice. *Geophysical Research Letters*, *35*(16), L16815. https://doi.org/10.1029/2008gl034536

Yang, X., Pyle, J. A., Cox, R. A., Theys, N., & Van Roozendael, M. (2010). Snow-sourced bromine and its implications for polar tropospheric ozone. *Atmospheric Chemistry and Physics*, *10*(16), 7763–7773. https://doi.org/10.5194/acp-10-7763-2010

Young, P. J., Naik, V., Fiore, A. M., Gaudel, A., Guo, J., Lin, M. Y., et al. (2018). Tropospheric Ozone Assessment Report: Assessment of global-scale model performance for global and regional ozone distributions, variability, and trends. *Elementa: Science of the Anthropocene*, *6*, 10. https://doi.org/10.1525/elementa.265

Zeng, G., Morgenstern, O., Williams, J. H. T., O'Connor, F. M., Griffiths, P. T., Keeble, J., et al. (2022). Attribution of stratospheric and tropospheric ozone changes between 1850 and 2014 in CMIP6 models. *Journal of Geophysical Research: Atmospheres*, *127*(16), e2022JD036452. https://doi.org/10.1029/2022JD036452

Zhang, J., Xie, F., Tian, W., Han, Y., Zhang, K., Qi, Y., et al. (2017). Influence of the Arctic Oscillation on the vertical distribution of wintertime ozone in the stratosphere and upper troposphere over the Northern Hemisphere. *Journal of Climate*, *30*(8), 2905–2919. https://doi.org/10.1175/JCLI-D-16-0651.1

Zilker, B., Richter, A., Blechschmidt, A.-M., von der Gathen, P., Bougoudis, I., Seo, S., et al. (2023). Investigation of meteorological conditions and BrO during ozone depletion events in Ny-Ålesund between 2010 and 2021 [preprint]. Atmospheric Chemistry and Physics Discussions. https://doi.org/10.5194/egusphere-2023-522

Erratum

In the originally published version of this article, coauthor Steven T. Turnock's first name was misspelled as "Stephen." The error has been corrected, and this may be considered the authoritative version of record.